Available online at www.sciencedirect.com
ScienceDirect
Icarus 193 (2008) 213–223
ICARUS
www.elsevier.com/locate/icarus

Tidal evolution of Mimas, Enceladus, and Dione

Jennifer Meyer *, Jack Wisdom

Massachusetts Institute of Technology, Cambridge, MA 02139, USA

Received 15 March 2007; revised 5 September 2007

Available online 3 October 2007

Abstract

The tidal evolution through several resonances involving Mimas, Enceladus, and/or Dione is studied numerically with an averaged resonance model. We find that, in the Enceladus–Dione 2:1 e-Enceladus type resonance, Enceladus evolves chaotically in the future for some values of k_2/Q. Past evolution of the system is marked by temporary capture into the Enceladus–Dione 4:2 ee'-mixed resonance. We find that the free libration of the Enceladus–Dione 2:1 e-Enceladus resonance angle of 1.5° can be explained by a recent passage of the system through a secondary resonance. In simulations with passage through the secondary resonance, the system enters the current Enceladus–Dione resonance close to tidal equilibrium and thus the equilibrium value of tidal heating of $1.1(18{,}000/Q_S)$ GW applies. We find that the current anomalously large eccentricity of Mimas can be explained by passage through several past resonances. In all cases, escape from the resonance occurs by unstable growth of the libration angle, sometimes with the help of a secondary resonance. Explanation of the current eccentricity of Mimas by evolution through these resonances implies that the Q of Saturn is below 100,000. Though the eccentricity of Enceladus can be excited to moderate values by capture in the Mimas–Enceladus 3:2 e-Enceladus resonance, the libration amplitude damps and the system does not escape. Thus past occupancy of this resonance and consequent tidal heating of Enceladus is excluded. The construction of a coherent history places constraints on the allowed values of k_2/Q for the satellites.

Keywords: Enceladus; Saturn, satellites; Satellites, dynamics; Resonances, orbital; Tides

1. Introduction

Enceladus poses a problem. Cassini observed active plumes emanating from Enceladus (Porco et al., 2006). The heat emanating from the south polar terrain is estimated to be 5.8 ± 1.9 GW (Spencer et al., 2006). Radiogenic heating is estimated to account for only 0.32 GW (Porco et al., 2006). The secondary spin–orbit model (Wisdom, 2004) could account for the heating, but the system was not found to be librating (Porco et al., 2006). The only remaining source of heating is tidal heating. Tidal heating in an equilibrium configuration, one in which the eccentricities no longer change as the semimajor axes continue to tidally evolve, can be estimated independent of satellite physical properties using conservation of angular momentum and energy. Equilibrium tidal heating can account for at most 1.1 GW of heating in Enceladus (Meyer and Wisdom, 2007a).

One possibility is that Enceladus is oscillating about the tidal equilibrium (Ojakangas and Stevenson, 1986). However, Meyer and Wisdom (2007b) have shown that for the physical parameters of Enceladus, the Ojakangas and Stevenson model does not oscillate. Another possibility is that the resonance is dynamically unstable. If the system exhibited a, perhaps temporary, episode of chaotic variations in the eccentricity then the heating rate could exceed the equilibrium heating rate. We have therefore undertaken a systematic exploration of the dynamics of the saturnian satellite system, focusing on the evolution of Enceladus. In particular, we study the evolution of Enceladus and Dione in the current 2:1 e-Enceladus type mean motion resonance. We also study the evolution of Mimas and Enceladus through the several 3:2 mean motion resonances.

Though our study was primarily motivated by Enceladus, the free eccentricity of 0.02 of Mimas also poses a problem. If primordial, it should have damped in the age of the Solar System. What excited it? To address this problem we have extended our study to include the Mimas–Dione 3:1 multiplet of resonances.

* Corresponding author.
E-mail address: meyerj@mit.edu (J. Meyer).

0019-1035/$ – see front matter
doi:10.1016/j.icarus.2007.09.008

2. Model

Our model is an averaged resonance model for a mean-motion commensurability between two coplanar satellites. We include all terms, both resonant and secular, in the disturbing function up to third order in the eccentricities of both satellites. We also model the oblateness of the planet, including J_2, J_4 and J_2^2 contributions. We include tidal evolution of the orbits and tidal damping of the eccentricities. The physical parameters, such as the Q_S of Saturn and the satellites, are all assumed to be constant in time. Details of the model are presented in Appendix A. We use the Bulirsch–Stoer algorithm to integrate the differential equations (Bulirsch and Stoer, 1966).

3. Equilibrium eccentricity

As a satellite system tidally evolves regularly into resonance, the eccentricity of one (or both) of the satellites grows because of the resonance interaction. As the eccentricity grows the dissipation grows with the square of the orbital eccentricity. Dissipation within a satellite tends to damp the orbital eccentricity. An equilibrium is possible: the satellites evolve deeper into the resonance, until the increase of eccentricity due to the evolution deeper into the resonance is balanced by the decrease of eccentricity due to internal dissipation.

When only the eccentricity of the interior satellite is excited the equilibrium eccentricity can be calculated (Meyer and Wisdom, 2007a):

$$e_0^2 = \frac{1}{7D_0}\left\{1 - \frac{1+m_1a_0/(m_0a_1)}{1+(m_1/m_0)\sqrt{a_1/a_0}} + \left(\frac{m_1}{m_0}\right)^2\left(\frac{a_0}{a_1}\right)^6\left[\frac{n_1}{n_0} - \frac{1+m_1a_0/(m_0a_1)}{1+(m_1/m_0)\sqrt{a_1/a_0}}\right]\right\}, \quad (1)$$

where a_i, m_i, and n_i are the semimajor axes, the masses, and the mean motions of the satellites (0 for interior, 1 for exterior), and where D_0 is a measure of the relative strength of tides in the interior satellite versus tides in Saturn:

$$D_0 = \frac{k_{2,0}}{Q_0}\frac{Q_S}{k_{2S}}\left(\frac{M_S}{m_0}\right)^2\left(\frac{R_0}{R_S}\right)^5. \quad (2)$$

Here $k_{2,0}$ and k_{2S} are the Love numbers, Q_0 and Q_S are the tidal dissipation factors, m_0 and M_S are the masses, and R_0 and R_S are the radii, of the interior satellite and Saturn, respectively. When only the eccentricity of the exterior satellite is excited then the equilibrium eccentricity is given by the same formula with the 0s and 1s interchanged.

As the equilibrium eccentricity is approached, the amplitude of libration in the resonance can either decrease or increase. It is either stable or unstable. In the case of Io in the Io–Europa 2:1 e-Io resonance, the libration amplitude damps and the equilibrium resonance configuration is stable. In the case of the evection resonance in the evolution of the Earth–Moon system, the libration amplitude grows as the equilibrium eccentricity is approached (Touma and Wisdom, 1998). This allows a natural escape from the resonance with an eccentricity near the equilibrium eccentricity. In our studies of the evolution of Mimas, Enceladus, and Dione, we found that sometimes the amplitude of libration damped and sometimes it grew, depending on the resonance and the physical parameters. Sometimes, as mentioned below, the escape from resonance is assisted by temporary capture into a secondary resonance, as occurred for Miranda (Tittemore and Wisdom, 1990).

After escape from resonance, the eccentricity decays with the timescale (Squyres et al., 1983)

$$\tau = \frac{2ma^5}{21nMR^5}\frac{Q}{k_2}, \quad (3)$$

where m is the satellite mass, a is the semimajor axis, n the mean motion, M the planet mass, R the satellite radius, Q the dissipation factor, and k_2 the satellite potential Love number. Note that the k_2/Q for the satellite affects both the equilibrium eccentricity (through the factor D_0) and the timescale for eccentricity damping.

4. Enceladus–Dione 2:1 e-Enceladus resonance—Future

Enceladus and Dione are currently in the Enceladus–Dione 2:1 e-Enceladus resonance.[1] Enceladus has a forced eccentricity of about 0.0047. The system has a free libration of about 1.5° (Sinclair, 1972). We decided to explore the future evolution of the system, with the primary goal of verifying the analytic predictions of the equilibrium eccentricity for various parameters. To our surprise, we found that the system exhibits complicated, sometimes (apparently) chaotic behavior.

The behavior we found depends on the assumed k_2/Q of Enceladus, which is unknown. So we made a systematic survey varying this parameter. We explored the range of k_2/Q between 1.8×10^{-5} to 9.4×10^{-4}. The lower bound corresponds to a Kelvin[2] $k_2 = 0.0018$ with a Q of 100. The upper bound corresponds roughly to a k_2 that is 10 times the Kelvin value with a Q of 20.

For $1.8 \times 10^{-5} < k_2/Q < 7.8 \times 10^{-5}$ the system tends toward the expected equilibrium, but as the eccentricity approaches the equilibrium eccentricity the libration amplitude increases. Eventually, the system escapes the resonance whereupon the eccentricity decays.

For $7.8 \times 10^{-5} < k_2/Q < 9.4 \times 10^{-5}$, the system exhibits an unexpected and interesting behavior. As in the previous case, the system tends toward equilibrium while the libration amplitude increases. Then the system enters a phase with large chaotic variations in the eccentricity while the resonance angle alternates between circulation and libration. Eventually the system escapes resonance and the eccentricity decays. After

[1] The resonant argument of the Enceladus–Dione 2:1 e-Enceladus resonance is $\lambda_E - 2\lambda_D + \varpi_E$, where λ_E and λ_D are the mean longitudes of Enceladus and Dione, and ϖ_E is the longitude of pericenter of Enceladus. For this resonance the eccentricity of Enceladus is excited.

[2] That is, using Kelvin's formula (Love, 1944)

$$k_2 = \frac{3/2}{1+19\mu/(2\rho g R)}$$

for the Love number of a homogeneous satellite of density ρ, radius R, surface gravity g, and rigidity μ. We chose $\mu = 4 \times 10^9$ N m^{-2}.

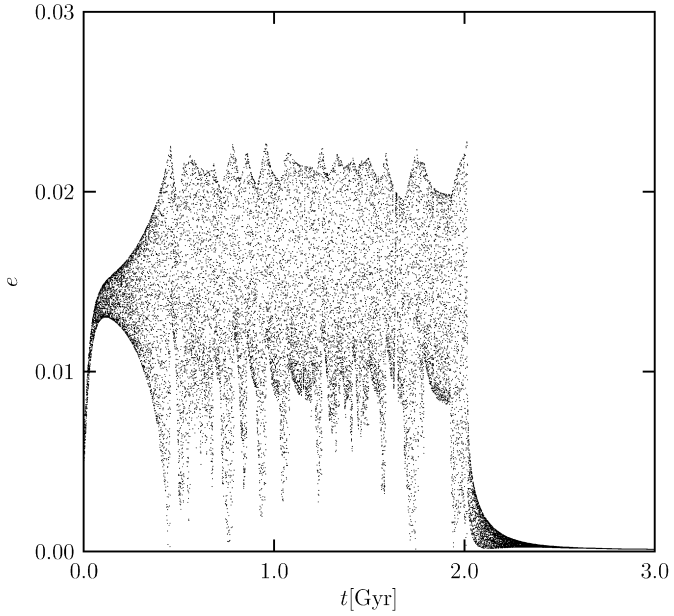

Fig. 1. The future evolution of Enceladus's eccentricity as it evolves deeper into the Enceladus–Dione 2:1 e-Enceladus resonance. The system approaches equilibrium, but the libration amplitude is unstable and the eccentricity enters a chaotic phase with large variations in amplitude. Eventually the system falls out of resonance. Here k_2/Q of Enceladus is 8.6×10^{-5}.

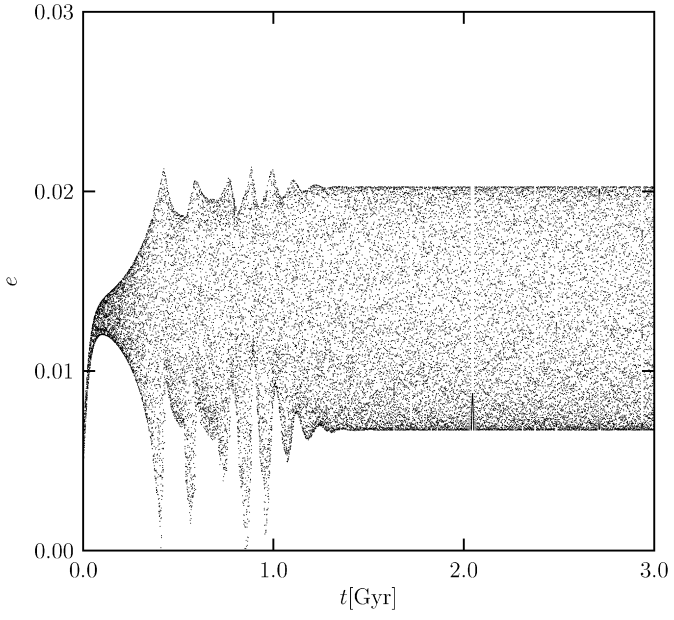

Fig. 2. The future evolution of Enceladus's eccentricity in the Enceladus–Dione 2:1 e-Enceladus type resonance for $k_2/Q = 1.0 \times 10^{-4}$. After the chaotic phase the system enters a limit cycle in which the eccentricity oscillates.

the system leaves the resonance the libration angle decays toward π. An example of this behavior is shown in Fig. 1.

For $9.4 \times 10^{-5} < k_2/Q < 1.76 \times 10^{-4}$, the system exhibits similar chaotic behavior to systems in the previous range of k_2/Q values, but the system ultimately does not escape the resonance. It settles into a finite amplitude librational equilibrium about the equilibrium eccentricity, as shown in Figs. 2–4. For

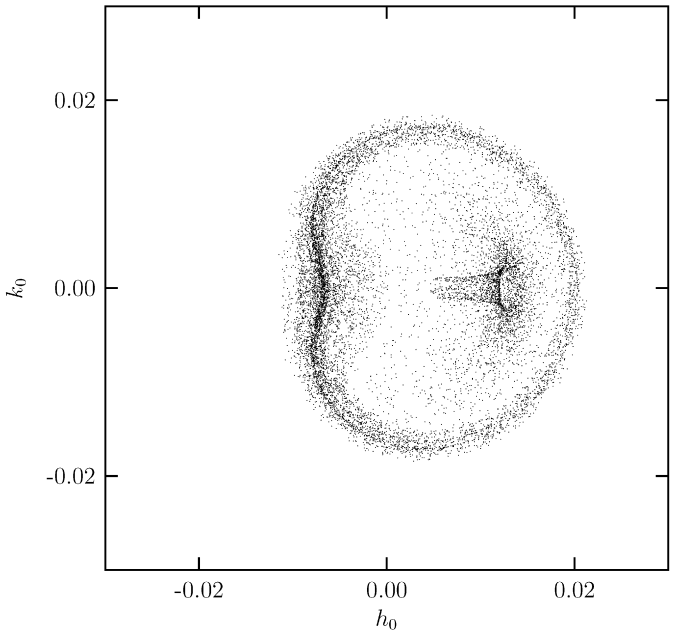

Fig. 3. The initial evolution, spanning 1.3 Gyr, for $k_2/Q = 1.0 \times 10^{-4}$ of that shown in Fig. 2 is shown in the phase plane $h_0 = e_0 \sin\sigma_0$ versus $k_0 = e_0 \cos\sigma_0$. The evolution begins with a libration near $\sigma_0 = 0$, the amplitude increases as the eccentricity increases. There is a chaotic transient which makes a splatter of points on the phase plane. The system eventually settles down on a limit cycle (see Fig. 5).

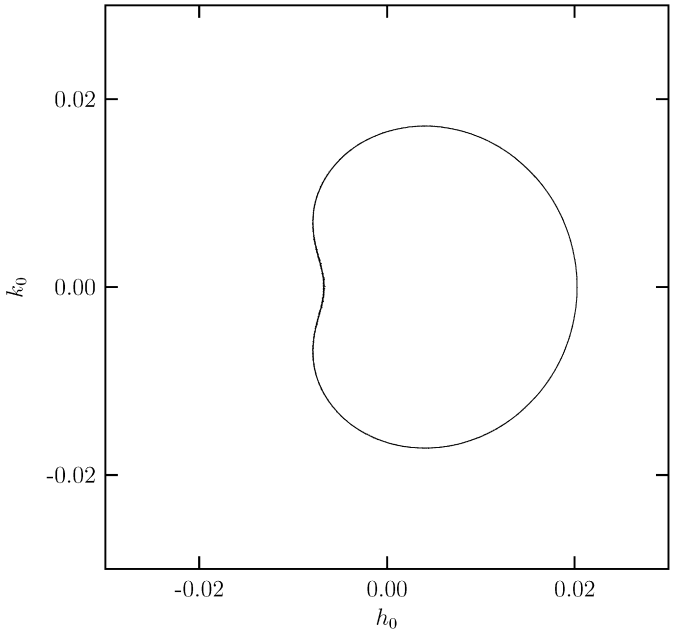

Fig. 4. The evolution of Enceladus in the Enceladus–Dione 2:1 e-Enceladus type resonance for $k_2/Q = 1.0 \times 10^{-4}$, eventually settles on a limit cycle, shown here in the phase plane $h_0 = e_0 \sin\sigma_0$ versus $k_0 = e_0 \cos\sigma_0$. The plotted segment of the orbit spans 3 Gyr.

larger values of k_2/Q, the chaotic phase is more brief. The fact that the evolution of the system settles on a limit cycle is interesting. We are unaware of other examples in which the endpoint of tidal evolution is a limit cycle.

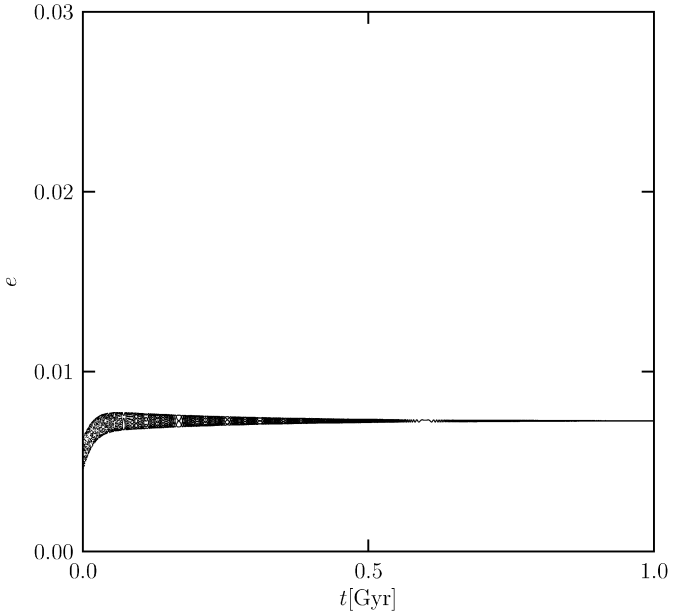

Fig. 5. The eccentricity of Enceladus in the Enceladus–Dione 2:1 e-Enceladus type resonance for $k_2/Q = 3.3 \times 10^{-4}$ reaches a stable equilibrium. The libration amplitude damps to zero.

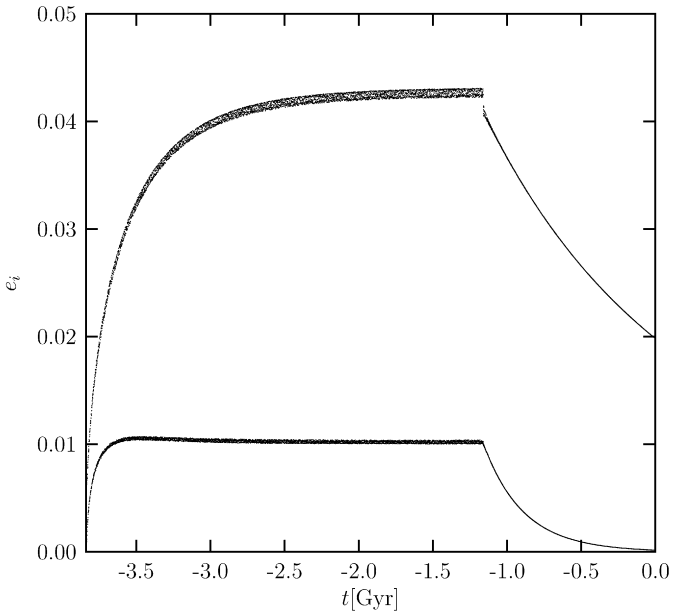

Fig. 6. The upper trace shows the evolution of the eccentricity of Mimas in the Mimas–Enceladus 6:4 mixed ee' resonance. The lower trace shows the evolution of the eccentricity of Enceladus. After leaving the resonance at -1.15 Gyr (for $Q_S = 18{,}000$), the eccentricity of Mimas decays to the current free eccentricity. Here k_2/Q for Mimas is 1.3×10^{-6}, and k_2/Q for Enceladus is 4.1×10^{-5}.

For $1.76 \times 10^{-4} < k_2/Q < 2.80 \times 10^{-4}$, the chaotic phase disappears, leaving a system that grows into stable finite amplitude libration about the equilibrium eccentricity.

For $k_2/Q > 2.80 \times 10^{-4}$, the eccentricity reaches a stable equilibrium and the libration amplitude damps to zero, as shown in Fig. 5. This behavior was observed up to $k_2/Q = 9.4 \times 10^{-4}$, but presumably extends beyond the studied range.

We have seen that a diverse range of behavior is possible for the future of the Enceladus–Dione resonance, depending on the unknown k_2/Q. In some of these scenarios, Enceladus has an exciting future.

5. Mimas–Enceladus 3:2 e-Enceladus resonance

One possible mechanism for heating Enceladus beyond the equilibrium limit is for Enceladus to evolve chaotically. The Enceladus–Dione 2:1 resonance exhibited such behavior in the future. The most recent first-order resonance that the system has passed through is the Mimas–Enceladus 3:2 e-Enceladus resonance, which was exited 1.16 Gyr ago (for a minimum Q_S of 18,000).[3] So we explored this resonance for similar chaotic behavior. However, we found regular evolution into equilibrium, with no excursions above equilibrium, chaotic or otherwise.

We examined the system for a range of k_2/Q of Enceladus of 6.0×10^{-6} to 9.4×10^{-4}. In order to assure capture into the e-Enceladus resonance,[4] we chose semimajor axes corresponding to a location just before the resonance and set the eccentricity of Enceladus to be 0.0011 so the capture probability was high. In every case, the system was captured into the e-Enceladus resonance and reached equilibrium. The libration amplitude damped. No escape or chaotic behavior was observed. We conclude that Enceladus was not captured into this resonance because we found no natural mechanism for escape.

6. Mimas–Enceladus 6:4 ee' resonance

The eccentricity of Mimas is relatively high (0.020) and has a short timescale for tidal decay. For a Q of 100 and a Kelvin k_2 of 0.00058, the timescale for decay of eccentricity is about 325 Myr. Thus, either the eccentricity of Mimas started at a much higher value, perhaps with a larger Q, or the eccentricity has been recently excited. The most recent first-order commensurability involving Mimas's eccentricity is the Mimas–Enceladus 3:2 mean-motion commensurability.

One of the resonances at the 3:2 mean-motion commensurability is the Mimas–Enceladus 6:4 ee'-mixed resonance, which was exited 1.15 Gyr ago (for Q_S of 18,000).[5] We examined evolution through this resonance as a possible explanation for Mimas's free eccentricity. We succeeded in explaining the current free eccentricity if Mimas's k_2/Q is 1.3×10^{-6}. The evolution of the eccentricities of Mimas and Enceladus is shown in Fig. 6.

[3] Using a constant Q_S model, Mimas would be at the synchronous radius at the beginning of the Solar System for approximately $Q_S = 18{,}000$ (Meyer and Wisdom, 2007a).

[4] The resonant argument of the Mimas–Enceladus 3:2 e-Enceladus resonance is $2\lambda_M - 3\lambda_E + \varpi_E$. For this resonance the eccentricity of Enceladus is excited.

[5] The resonant argument of the Mimas–Enceladus 6:4 ee'-mixed resonance is $4\lambda_M - 6\lambda_E + \varpi_M + \varpi_E$. For this resonance the eccentricities of both Mimas and Enceladus are excited.

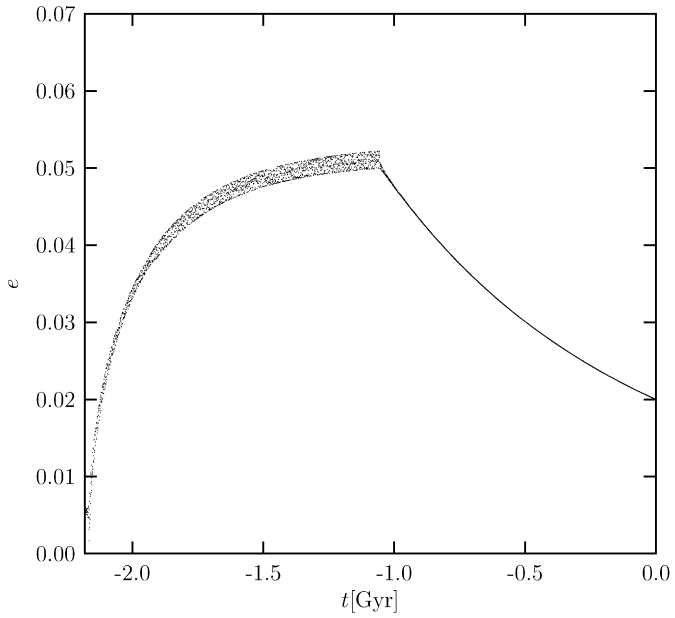

Fig. 7. The evolution of the eccentricity of Mimas as it encounters the Mimas–Enceladus 3:2 e-Mimas resonance. The eccentricity approaches an equilibrium value of 0.052, but as it reaches equilibrium, the libration amplitude grows. Eventually the system escapes from the resonance and the eccentricity decays to the current value at the present. Here k_2/Q of Mimas is 1.42×10^{-6} and the timescale for eccentricity decay is about 1.3 Gyr.

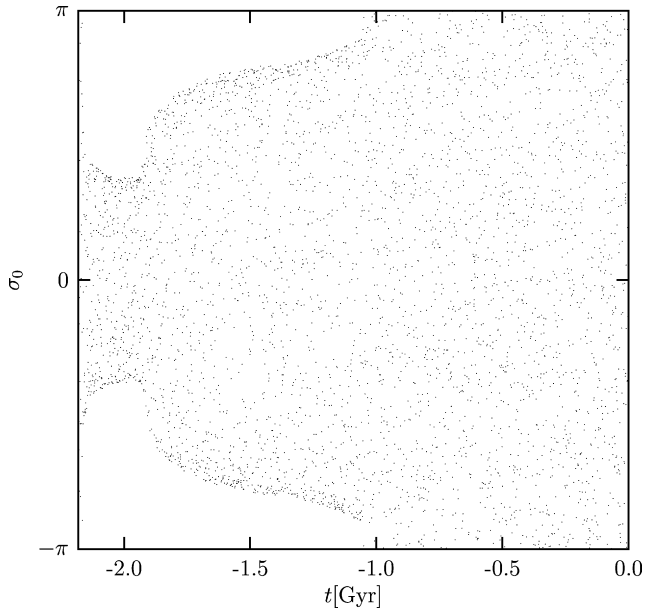

Fig. 8. The resonance angle of the Mimas–Enceladus 3:2 e-Mimas resonance versus time. There is a sudden growth in the libration amplitude because the system was captured by a 3-fold secondary resonance. When the amplitude reaches π, the system falls out of resonance. This figure corresponds to Fig. 10.

The time of exit from the resonance depends upon the Q of Saturn, which is here taken to be the minimum $Q_S = 18{,}000$. For larger Q_S the required k_2/Q of Mimas would be smaller.

7. Mimas–Enceladus 3:2 e-Mimas resonance

Another of the multiplet of resonances at this mean-motion commensurability is the Mimas–Enceladus 3:2 e-Mimas resonance,[6] which was exited 1.14 Gyr ago (for a minimum Q of Saturn of $Q_S = 18{,}000$).

We also examined evolution through this resonance to see whether Mimas's eccentricity can be explained. We found that Mimas's eccentricity could be explained and that there exists an intrinsic dynamical mechanism of escape from the resonance. In particular, the libration amplitude grows until the amplitude of the libration reaches π whereupon the system falls out of resonance.

For a k_2/Q of 1.42×10^{-6} for Mimas, Fig. 7 shows the evolution of eccentricity toward an equilibrium value of 0.052, followed by a period in which the variations of the eccentricity grow larger, and then as the system escapes from the resonance the eccentricity decays to the present value at the current time. This particular k_2/Q was chosen so that Mimas's eccentricity would damp to the current value at the present from the equilibrium eccentricity at the time at which the system left the resonance. This exit time depends upon the Q of Saturn, which is here taken to be the minimum $Q_S = 18{,}000$. For larger Q_S the required k_2/Q of Mimas would be smaller.

Fig. 8 shows the resonance angle for this resonance. The libration amplitude shows a sudden increase as the system is caught in a 3-fold secondary resonance, between the libration frequency and the frequency of circulation of σ_1. This is similar to the mechanism that took Miranda out of resonance at an inclination near 4° (Tittemore and Wisdom, 1990).

Mimas's eccentricity can be explained either by passage through the 3:2 e-Mimas resonance, or the 6:4 ee'-mixed resonance. Placing these resonances at the birth of the Solar System limits the time-averaged Q of Saturn to be below 70,000.[7]

8. Mimas–Dione 3:1 resonance

As discussed in the following section on the past evolution into the Enceladus–Dione 2:1 resonance, the eccentricity of Dione is required to exceed 0.001 at the time the system encounters the Enceladus–Dione 2:1 e-Dione resonance. The most likely mechanism for exciting the eccentricity of Dione is temporary capture into the Mimas–Dione 3:1 ee'-mixed resonance. In addition, capture into this resonance is another possible explanation for the current free eccentricity of Mimas. Passage through this resonance occurred 0.75 Gyr ago, for a Q_S of 18,000, after passage through the Mimas–Enceladus 3:2 resonance.

Another possible explanation of Mimas's free eccentricity is the Mimas–Dione 3:1 e^2-Mimas resonance, which occurred 0.70 Gyr ago, for a Q_S of 18,000. A representative evolution through this resonance is shown in Fig. 9. In this resonance, the eccentricity of Dione is not excited. The former explanation of

[6] The resonant argument of the Mimas–Enceladus 3:2 e-Mimas resonance is $2\lambda_M - 3\lambda_E + \varpi_M$. For this resonance the eccentricity of Mimas is excited.

[7] Q_S may be non-constant—our calculations place limits on only the integrated evolution.

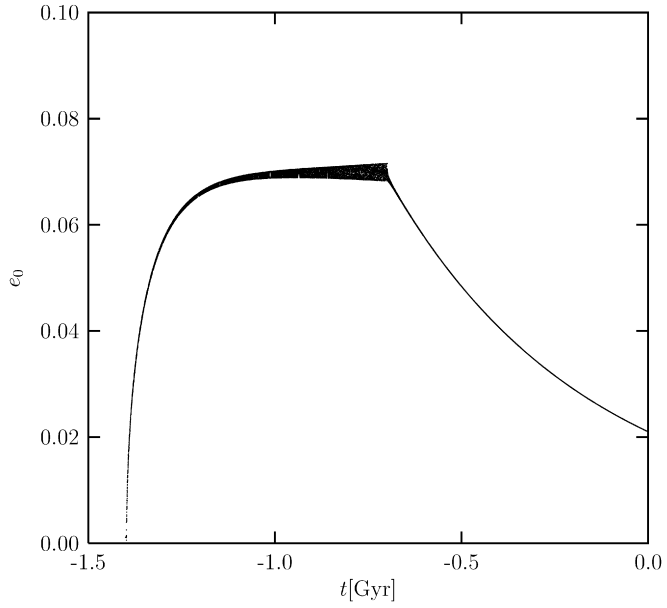

Fig. 9. The evolution of the eccentricity of Mimas as it encounters the Mimas–Dione 3:1 e^2-Mimas resonance. The eccentricity grows to an equilibrium value of 0.07 before escaping the resonance and decaying to the present value of 0.02. Escape from the resonance occurs via unstable growth of the libration amplitude. Here k_2/Q for Mimas is 3.0×10^{-6}.

the eccentricity of Mimas is preferred because it also excites the eccentricity of Dione.

Explaining Mimas's eccentricity via either of these resonances places an upper limit on the Q of Saturn of 100,000 (placing this resonance at the birth of the Solar System). To reach the current eccentricity of Mimas at the present time requires a k_2/Q of Mimas of 3.0×10^{-6} in the e^2-Mimas resonance or a k_2/Q of Mimas of 2.6×10^{-6} in the ee'-mixed resonance.

9. Enceladus–Dione 2:1 *e*-Enceladus resonance—Past

For an isolated first-order e-type resonance, the tidal evolution into the resonance is simple. But when more than one resonance is present, the evolution can be more complicated, even though the multiplet of resonances associated with a commensurability are split due to the oblateness of the planet. The evolution of the Enceladus and Dione through the multiplet of resonances associated with the 2:1 commensurability has been the subject of some discussion (Sinclair, 1983; Peale, 1986). Here we study the evolution numerically.

We have carried out an extensive survey of the evolution of the system through the multiplet of eccentricity-type resonances associated with the 2:1 commensurability between Enceladus and Dione. We found that the evolution of the system was more complicated than expected. In particular, we found that it was rather difficult for the system to pass through the other resonances of the multiplet before being finally captured in the current resonance. The third-order Enceladus–Dione 6:3 $ee'e'$-mixed resonance[8] is surprisingly important in the evolution. Also important is the Enceladus–Dione 4:2 ee'-mixed resonance.[9]

In our simulations the system was initially captured by the Enceladus–Dione 2:1 e-Enceladus resonance, before any of the other resonances of the multiplet were encountered. As the system subsequently passed through the Enceladus–Dione e-Dione resonance, it was occasionally captured. However, once captured, the libration amplitude damps and precludes a natural escape from the resonance; we conclude that the system was not captured into this resonance. The next resonance encountered (in our model) is the third-order $ee'e'$ resonance. We found that the system was easily captured into this resonance, and that once captured the system had no natural mechanism for escape. In rare cases, when the eccentricity of Dione was near the critical value for certain capture, the system did escape this resonance by unstable growth of the libration amplitude. But it is likely that this resonance was avoided by the actual system. We found that in order to avoid capture into this resonance the eccentricity of Dione had to exceed about 0.001 at the time of e-Dione resonance encounter. (For one mechanism to explain this eccentricity, see above.) We also found that successful passage through the third-order resonance required that k_2/Q of Dione be in certain ranges, depending on the eccentricity of Dione at the time of the e-Dione resonance encounter. For $e_D = 0.001$, we found k_2/Q needs to be smaller than about 1.4×10^{-5}. For $e_D = 0.003$, we found that k_2/Q for Dione needs to be less than 8.8×10^{-5}.

Once the system avoids the third-order resonance, then in our simulations it is almost always captured by the ee'-mixed resonance (in only one case out of hundreds the system passed through the mixed resonance without being captured). However, unlike the third-order resonance, in this resonance the libration amplitude is always unstable and the system naturally escapes. As it escapes we found that it falls directly into the e-Enceladus resonance.

As the system falls into the e-Enceladus resonance the system exhibits all the behavior catalogued in Section 4. But the limiting behavior happens right away; the system does not fall out of the resonance with an eccentricity much below the equilibrium value. In a survey of the possible behavior as a function of the k_2/Q for Enceladus, we only found a behavior consistent with the current state of the system if k_2/Q was at or just below the equilibrium value of k_2/Q.[10] The equilibrium value is 8×10^{-4}; we found values as low as 4.8×10^{-4} also passed through the current state of the system. But usually, we found the system escaped near the equilibrium value for a given k_2/Q. These results suggest that k_2/Q for Enceladus is closer to the equilibrium value than the Kelvin value (even with a Q as low as 20). For values of k_2/Q near the equilibrium value, the libration amplitude damps in a few tens of millions of years once

[8] The resonant argument of the Enceladus–Dione 6:3 $ee'e'$-mixed resonance is $3\lambda_E - 6\lambda_D + \varpi_E + 2\varpi_D$.

[9] The resonant argument of the Enceladus–Dione 4:2 ee'-mixed resonance is $2\lambda_E - 4\lambda_D + \varpi_E + \varpi_D$.

[10] By "equilibrium value" of k_2/Q we mean the value such that the current state of the system is at a tidal equilibrium, that is, the eccentricity is no longer changing. See Meyer and Wisdom (2007a).

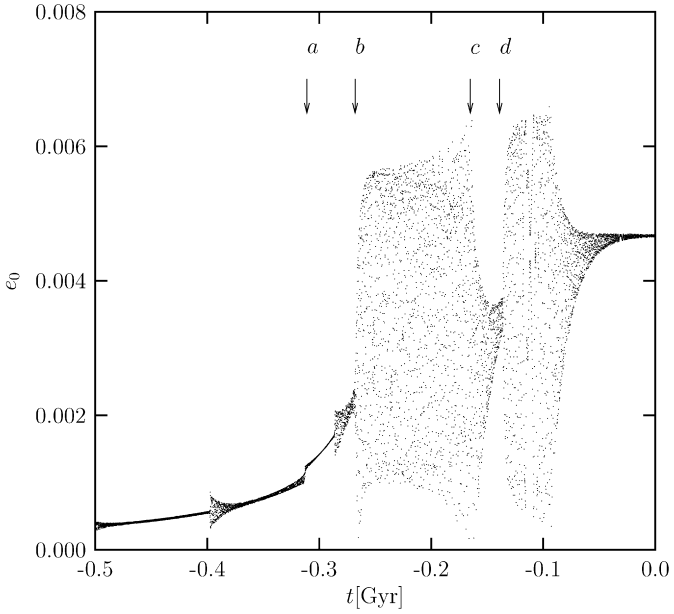

Fig. 10. The past evolution of the eccentricity of Enceladus in the Enceladus–Dione 2:1 multiplet of resonances. Feature 'b' shows the entrance into the ee' resonance and feature 'd' shows capture into a 2:1 secondary resonance. In this simulation, the k_2/Q of Enceladus is the equilibrium value of 8.0×10^{-4}, so the constant equilibrium eccentricity of Enceladus, which it achieves shortly after it leaves the secondary resonance, is the current value of 0.0047.

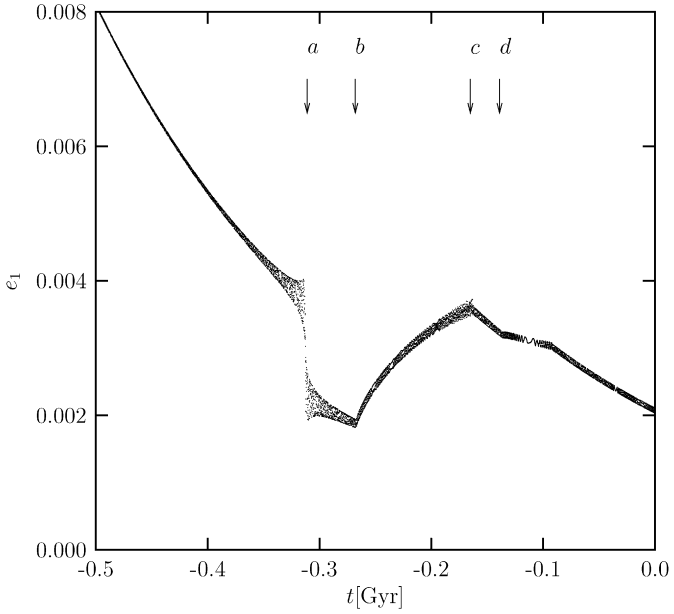

Fig. 11. The past evolution of the eccentricity of Dione in the Enceladus–Dione 2:1 multiplet of resonances. Feature 'a' shows passage through the e-Dione resonance. The rise in eccentricity between events 'b' and 'c' is due to the ee'-mixed resonance. The value of k_2/Q of Dione is 1.24×10^{-4}.

it enters the e-Enceladus resonance. Since the eccentricity of Dione needs to decay to its current value, this rapid decay of the libration amplitude may be inconsistent with the current state of the system.

However, we found that once the system is in the e-Enceladus resonance, it is often temporarily captured in a 2:1 secondary resonance between the libration frequency and the frequency of circulation of the e-Dione resonance angle (σ_1).[11] The system escapes the secondary resonance by unstable growth of the secondary resonance libration angle. Once out of the secondary resonance, the libration amplitude in the e-Enceladus resonance damps. The current libration amplitude is probably evidence that the system has recently passed through this secondary resonance. This allows time for the eccentricity of Dione to damp to its current value.

The evolution of the eccentricities of Enceladus and Dione as the system evolves through the Enceladus–Dione 2:1 multiplet of resonances are shown in Figs. 10 and 11, respectively. In this simulation, the k_2/Q of Enceladus is 8.0×10^{-4}, the value for which the current eccentricity is the equilibrium eccentricity. The k_2/Q of Dione is 1.24×10^{-4}. The event marked 'a' shows passage through the e-Dione resonance. Event 'b' is capture into the ee'-mixed resonance. Escape from the ee'-mixed resonance ('c') is quickly followed by capture into the 2:1 secondary resonance ('d').

[11] After this work was nearly complete we learned of the work of Callegari and Yokoyama (2007), who noted the existence of secondary resonances in this system.

10. Discussion

The values of k_2/Q for the satellites in the above sections were calculated for a minimum Q_S of 18,000. For a maximum Q_S that places the resonances at the beginning of the Solar System, the values of k_2/Q are smaller. We can estimate the required values of k_2/Q by assuming that the eccentricity upon exiting the resonance is approximately the equilibrium eccentricity. We then constrain k_2/Q for each satellite by the requirement that the eccentricity decay to the present value at the present time. Fig. 12 shows the values of k_2/Q, determined in this way, for Mimas as a function of Q_S, for the Mimas–Enceladus 3:2 e-Mimas resonance and for the Mimas–Dione 3:1 e^2-Mimas resonance.

We see that, as expected, a larger Q_S requires a smaller k_2/Q for Mimas. Basically, this is because the time since exiting the resonance is longer for a larger Q_S and to slow the decay of the eccentricity k_2/Q must be smaller. The k_2/Q for Mimas in the Mimas–Enceladus 3:2 resonance is smaller than that in the Mimas–Dione 3:1 resonance. The 3:1 resonance occurs closer to the present time, so the eccentricity must damp more quickly, and also the 3:1 equilibrium eccentricity is larger than the 3:2 equilibrium eccentricity.

The interpretation of these values of k_2/Q depends on the assumed rigidity through the Love number k_2. The rigidity of ice (and rock) at the conditions of Mimas is uncertain. In computing the Kelvin value of the Love number presented above, we used a rigidity of $4 \times 10^9\ \mathrm{N\,m^{-2}}$. With this rigidity, the Kelvin k_2 of Mimas is 5.8×10^{-4}. Thus the required Q of Mimas for the free eccentricity of Mimas to be explained by passage through the Mimas–Dione 3:1 e^2-Mimas resonance ranges from about 190 (for Q_S of 18,000) to about 1000 (for $Q_S = 100{,}000$). The required Q for Mimas for the Mimas–

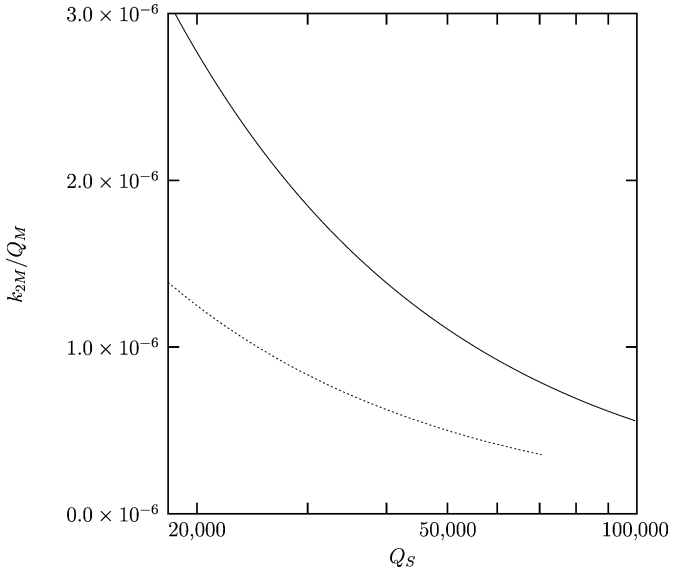

Fig. 12. The solid line shows the k_2/Q for Mimas for which the eccentricity of Mimas will decay to the current value for a given Q_S if the system was caught in the Mimas–Dione 3:1 e^2-Mimas resonance. The dotted line shows the k_2/Q for Mimas for which the eccentricity of Mimas will decay to the current value for a given Q_S if the system was caught in the Mimas–Enceladus 3:2 e-Mimas resonance.

Dione 3:1 ee'-mixed resonance ranges from about 220 (for Q_S of 18,000) to about 1050 (for Q_S of 100,000). The required Q for Mimas for the Mimas–Enceladus 3:2 resonance ranges from about 420 (for Q_S of 18,000) to about 1600 (for Q_S of 70,000). But these values of Q are uncertain because of uncertainties in the Love number. First, the rigidity assumed may be uncertain by up to a factor of 3 in both directions (Moore, 2004). Then there may be viscoelastic modification of the "dynamic" Love number (Ross and Schubert, 1989). With these uncertainties, the required values of Q should not be taken too literally. Nevertheless, some may be uncomfortable with the large Q of Mimas required at the larger Q_S end of the allowed range. This might suggest that Q_S is closer to 18,000 than 100,000.

11. Conclusion

We have numerically explored tidal evolution through several resonances, including the multiplets of the Enceladus–Dione 2:1 resonance, the Mimas–Enceladus 3:2 resonance, and the Mimas–Dione 3:1 resonance.

Enceladus may have an interesting future in the Enceladus–Dione 2:1 e-Enceladus resonance. For a range of k_2/Q, we found that the system exhibits complicated and sometimes chaotic behavior. Unfortunately, we only found this interesting behavior in the future. Therefore, such chaotic episodes cannot explain the current heating of Enceladus.

We then investigated the past Mimas–Enceladus 3:2 e-Enceladus resonance to see if similar chaotic episodes occurred. We found no chaotic behavior and moreover, no natural dynamical mechanism for escape. If the system had been captured in this resonance, it would have remained in the resonance until the present time, contrary to its observed state.

We found multiple possible explanations for the large free eccentricity of Mimas. The Mimas–Enceladus 6:4 ee'-mixed resonance can explain Mimas's current free eccentricity of 0.020 for a k_2/Q of Mimas of about 1.3×10^{-6}. Escape from this resonance is by growth of the libration amplitude.

In addition, the Mimas–Enceladus 3:2 e-Mimas resonance can excite Mimas's eccentricity to large values, and for a k_2/Q of about 1.42×10^{-6}, the eccentricity can decay from values near the equilibrium value of 0.052 to the current value in the 1.14 Gyr since the resonance was exited (for $Q_S = 18{,}000$). The system escapes as the libration amplitude grows to π, sometimes with the help of temporary capture in a secondary resonance.

If Mimas's eccentricity is explained by either of the above mechanisms, the time-averaged Q of Saturn is constrained to be less than 70,000 so that the Mimas–Enceladus 3:2 resonance multiplet occurs after the birth of the Solar System.

Mimas's eccentricity could also be explained via excitation in the Mimas–Dione 3:1 e^2-Mimas resonance for a k_2/Q of Mimas of 3.0×10^{-6} or the Mimas–Dione 3:1 ee'-mixed resonance for a k_2/Q of Mimas of 2.6×10^{-6}. In these cases, the time-averaged Q of Saturn is constrained to be less than 100,000.

Of the Mimas–Enceladus 6:4 ee'-mixed resonance, the Mimas–Enceladus 3:2 e-Mimas resonance, the Mimas–Dione 3:1 e^2-Mimas resonance, and the Mimas–Dione 3:1 ee'-mixed resonance, the Mimas–Enceladus 6:4 ee'-mixed resonance is encountered first as Mimas tidally evolves. If it is captured then the eccentricity of Mimas will be large after escape, so subsequent capture into the Mimas–Enceladus 3:2 e-Mimas resonance will be unlikely (we estimate 1.4% using the formulae of Borderies and Goldreich, 1984). If the eccentricity decays sufficiently, then there is a chance that the system will be subsequently captured into the Mimas–Dione 3:1 e^2-Mimas resonance or the Mimas–Dione 3:1 ee'-mixed resonance. For a maximum k_2/Q for Mimas of 3×10^{-6} we estimate the probability of this capture in the 3:1 resonance at 4.5%. Alternatively, the system may pass through the Mimas–Enceladus 6:4 ee'-mixed resonance, and be captured into the Mimas–Enceladus 3:2 e-Mimas resonance. After escape, the system again has a small chance of being captured by one of the Mimas–Dione 3:1 resonances. Capture into the Mimas–Dione 3:1 ee'-mixed resonance is preferred because the scenario requires lower (perhaps more realistic) Q of Mimas and also excites the eccentricity of Dione to the level required for successful passage through the Enceladus–Dione 2:1 multiplet.

The evolution into the current Enceladus–Dione 2:1 e-Enceladus resonance is surprisingly complicated. The system is first captured into the e-Enceladus resonance, well before the point of exact commensurability. Subsequent evolution is marked by passage through the e-Dione, $ee'e'$-, and ee'-mixed resonances. In order to successfully arrive at the current state of the system, the e-Dione and $ee'e'$ resonances must be avoided because once captured, escape is unlikely. In our simulations, we found that this requires that the eccentricity of Dione must exceed 0.001 when it encounters the e-Dione resonance.

A likely mechanism for exciting the eccentricity of Dione is capture into the Mimas–Dione 3:1 ee'-mixed resonance.

Once the system has passed the e-Dione and $ee'e'$-mixed resonances, the system is usually captured into the Enceladus–Dione 2:1 ee'-mixed resonance and this phase of the evolution shows large variations in the eccentricity of Enceladus. However, these variations are unfortunately not large enough to substantially enhance the heating rate over the equilibrium rate. The system naturally escapes the ee'-mixed resonance by growth of the libration amplitude, and then is immediately captured back into the e-Enceladus resonance.

After leaving the ee'-mixed resonance, the system usually is caught in a 2:1 secondary resonance between the libration frequency in the e-Enceladus resonance and the circulation frequency of the e-Dione resonance angle. This secondary resonance temporarily increases the libration amplitude of the e-Enceladus resonance angle. In some of our simulations, the e-Enceladus libration amplitude damped to the current observed value of 1.5° as the eccentricity of Dione damped to its observed value of 0.0022.

Since the system always escapes this secondary resonance close to equilibrium, we are able to conclude that Enceladus is probably near its equilibrium eccentricity. Therefore the equilibrium heating rate of $1.1(18{,}000/Q_S)$ GW (Meyer and Wisdom, 2007a) due to Enceladus–Dione 2:1 e-Enceladus resonance applies. To exceed this rate of heating requires some form of non-equilibrium behavior.

Acknowledgments

Some of the numerical simulations for this research were performed on Caltech's Division of Geological and Planetary Sciences Dell cluster. This research was supported in part by the NASA Planetary Geology and Geophysics Program.

Appendix A

We derived our model in a Hamiltonian framework and then added dissipative terms. While terms up to third order in eccentricity were included in our model, we present only second order terms here. The Hamiltonian is

$$H = H_K + H_J + H_s + H_r, \tag{A.1}$$

where H_K is the sum of the Kepler Hamiltonians for all the satellites, H_J is the Hamiltonian for the oblateness contributions, H_s is the secular Hamiltonian, H_r is the resonant Hamiltonian, which has both direct and indirect contributions. Each of these is initially expressed in Jacobi coordinates to effect the elimination of the center of mass (Wisdom and Holman, 1991). We then reexpress each term in terms of canonical Delaunay and then modified Delaunay elements. Finally, we make a polar canonical transformation (Sussman and Wisdom, 2001) on each pair of eccentricity-like momenta and conjugate coordinates to get coordinates that are nonsingular at small eccentricity. The individual steps will not be shown in detail.

The state variables are as follows:

$$h_i = e_i \cos\sigma_i, \tag{A.2}$$

$$k_i = e_i \sin\sigma_i, \tag{A.3}$$

$$\tilde{a}_i = \Lambda_i^2/m_i\mu_i, \tag{A.4}$$

where we label the satellites with subscript $i = 0$ for the inner satellite and $i = 1$ for the outer satellite in the resonant pair. The mass of satellite i is m_i, and $\mu_i = Gm_iM$, where M is the planet mass. The eccentricity of satellite i is e_i. The resonance variables are $\sigma_i = j\lambda_1 + (1-j)\lambda_0 - \varpi_i$, where λ_i and ϖ_i are the mean longitude and longitude of pericenter of satellite i. We also have

$$\Lambda_0 = L_0 - (1-j)(\Sigma_0 + \Sigma_1), \tag{A.5}$$

$$\Lambda_1 = L_1 - j(\Sigma_0 + \Sigma_1), \tag{A.6}$$

where $L_i = \sqrt{m_i\mu_i a_i}$, for semimajor axis a_i, and

$$\Sigma_i = \sqrt{m_i\mu_i a_i}\left(1 - \left(1 - e_i^2\right)^{1/2}\right) \approx \Lambda_i e_i^2/2, \tag{A.7}$$

where $L_i \approx \Lambda_i$ to first order in eccentricity. We define $\Sigma_i = \Lambda_i\bar{\Sigma}_i$. Note that in the absence of tides the state variables $\tilde{a}_i$ and the associated variables Λ_i are constants of the motion. The osculating semimajor axes a_i and the associated L_i are not constant.

Let

$$\frac{\partial H_K}{\partial \Sigma_i} = (1-j)n_0 + jn_1, \tag{A.8}$$

where the mean motions are $n_0 = m_0\mu_0^2/L_0^3$ and $n_1 = m_1\mu_1^2/L_1^3$. We also define $\tilde{n}_0 = m_0\mu_0^2/\Lambda_0^3$ and $\tilde{n}_1 = m_1\mu_1^2/\Lambda_1^3$. In terms of these, we define

$$\Delta n_0 = \tilde{n}_0\left(3\frac{J_2R^2}{\tilde{a}_0^2} + \frac{45}{4}\frac{J_2^2R^4}{\tilde{a}_0^4} - \frac{15}{4}\frac{J_4R^4}{\tilde{a}_0^4}\right), \tag{A.9}$$

$$\Delta n_1 = \tilde{n}_1\left(3\frac{J_2R^2}{\tilde{a}_1^2} + \frac{45}{4}\frac{J_2^2R^4}{\tilde{a}_1^4} - \frac{15}{4}\frac{J_4R^4}{\tilde{a}_1^4}\right), \tag{A.10}$$

$$\Delta\dot{\varpi}_0 = \tilde{n}_0\left(\frac{3}{2}\frac{J_2R^2}{\tilde{a}_0^2} + \frac{63}{8}\frac{J_2^2R^4}{\tilde{a}_0^4} - \frac{15}{4}\frac{J_4R^4}{\tilde{a}_0^4}\right), \tag{A.11}$$

$$\Delta\dot{\varpi}_1 = \tilde{n}_1\left(\frac{3}{2}\frac{J_2R^2}{\tilde{a}_1^2} + \frac{63}{8}\frac{J_2^2R^4}{\tilde{a}_1^4} - \frac{15}{4}\frac{J_4R^4}{\tilde{a}_1^4}\right). \tag{A.12}$$

These are the changes in the mean motions and the changes in the rates of precession of the pericenters due to planetary oblateness (Brouwer, 1959).

Next we define

$$\Delta\dot{\sigma}_0 = (1-j)\Delta n_0 + j\Delta n_1 - \Delta\dot{\varpi}_0 \tag{A.13}$$

and

$$\Delta\dot{\sigma}_1 = (1-j)\Delta n_0 + j\Delta n_1 - \Delta\dot{\varpi}_1. \tag{A.14}$$

These are the changes in the rates of change of the resonant arguments due to planetary oblateness.

The equations of motion are as follows:

$$\begin{aligned}\frac{\mathrm{d}k_0}{\mathrm{d}t} = {}& \frac{\partial H_K}{\partial \Sigma_0}h_0 + \Delta\dot{\sigma}_0 h_0 \\ & - \frac{Gm_0m_1}{\tilde{a}_1\Lambda_0}\left(C^s_{ee'}h_1 + 2C^s_{ee}h_0 + C^r_e\right. \\ & \left. + 2C^r_{ee}h_0 + C^r_{ee'}h_1\right) + \left.\frac{\mathrm{d}k_0}{\mathrm{d}t}\right|_t,\end{aligned} \tag{A.15}$$

$$\frac{\mathrm{d}h_0}{\mathrm{d}t} = -\frac{\partial H_K}{\partial \Sigma_0}k_0 - \Delta\dot{\sigma}_0 k_0 - \frac{Gm_0m_1}{\tilde{a}_1\Lambda_0}\big(-C^s_{ee'}k_1 - 2C^s_{ee}k_0 + 2C^r_{ee}k_0 + C^r_{ee'}k_1\big) + \left.\frac{\mathrm{d}h_0}{\mathrm{d}t}\right|_t, \tag{A.16}$$

$$\frac{\mathrm{d}k_1}{\mathrm{d}t} = \frac{\partial H_K}{\partial \Sigma_1}h_1 + \Delta\dot{\sigma}_1 h_1 - \frac{Gm_0m_1}{\tilde{a}_1\Lambda_1}\big(2C^s_{e'e'}h_1 + C^s_{ee'}h_0 + C^r_{e'} + 2C^r_{e'e'}h_1 + C^r_{ee'}h_0\big) + \left.\frac{\mathrm{d}k_1}{\mathrm{d}t}\right|_t, \tag{A.17}$$

$$\frac{\mathrm{d}h_1}{\mathrm{d}t} = -\frac{\partial H_K}{\partial \Sigma_1}k_1 - \Delta\dot{\sigma}_1 k_1 - \frac{Gm_0m_1}{\tilde{a}_1\Lambda_1}\big(-2C^s_{e'e'}k_1 - C^s_{ee'}k_0 + 2C^r_{e'e'}k_1 + C^r_{ee'}k_0\big) + \left.\frac{\mathrm{d}h_1}{\mathrm{d}t}\right|_t. \tag{A.18}$$

The tidal damping terms for satellite i are

$$\left.\frac{\mathrm{d}k_i}{\mathrm{d}t}\right|_t = -\frac{7}{2}c_i D_i a_i^{-13/2}k_i\eta, \tag{A.19}$$

$$\left.\frac{\mathrm{d}h_i}{\mathrm{d}t}\right|_t = -\frac{7}{2}c_i D_i a_i^{-13/2}h_i\eta, \tag{A.20}$$

where

$$c_i = 3\frac{k_2}{Q}\frac{m_0}{M}\sqrt{GM}R^5 \tag{A.21}$$

and

$$D_i = \frac{k_{2i}/Q_i}{k_2/Q}\left(\frac{M}{m_i}\right)^2\left(\frac{R_i}{R}\right)^5. \tag{A.22}$$

The factor η is a "speedup" factor that artificially enhances the rate of tidal evolution. We found in selected test evolutions that the evolution was insensitive to the speedup factor over a range of speedups of 1 to 1000. We typically used a speedup of 100 in our numerical explorations.

The tidal contribution to the rate of change of semimajor axis a_i is

$$\left.\frac{\mathrm{d}a_i}{\mathrm{d}t}\right|_t = c_i\big(1 - 7D_i e_i^2\big)a^{-11/2}\eta. \tag{A.23}$$

From $L_i = \sqrt{m_i\mu_i a_i}$ we have

$$\dot{L}_i^t = \left.\frac{\mathrm{d}L_i}{\mathrm{d}t}\right|_t = \frac{L_i}{2a_i}\left.\frac{\mathrm{d}a_i}{\mathrm{d}t}\right|_t. \tag{A.24}$$

From $\bar{\Sigma}_i = (h_i^2 + k_i^2)/2$ we have

$$\dot{\bar{\Sigma}}_i^t = \left.\frac{\mathrm{d}\bar{\Sigma}_i}{\mathrm{d}t}\right|_t = h_i\left.\frac{\mathrm{d}h_i}{\mathrm{d}t}\right|_t + k_i\left.\frac{\mathrm{d}k_i}{\mathrm{d}t}\right|_t. \tag{A.25}$$

From the definitions

$$\Lambda_0 = L_0 - (1-j)(\Lambda_0\bar{\Sigma}_0 + \Lambda_1\bar{\Sigma}_1), \tag{A.26}$$

$$\Lambda_1 = L_1 - j(\Lambda_0\bar{\Sigma}_0 + \Lambda_1\bar{\Sigma}_1) \tag{A.27}$$

we differentiate to get

$$\dot{\Lambda}_0^t = \dot{L}_0^t - (1-j)\big(\dot{\Lambda}_0^t\bar{\Sigma}_0 + \dot{\Lambda}_1^t\bar{\Sigma}_1 + \Lambda_0\dot{\bar{\Sigma}}_0^t + \Lambda_1\dot{\bar{\Sigma}}_1^t\big), \tag{A.28}$$

$$\dot{\Lambda}_1^t = \dot{L}_1^t - j\big(\dot{\Lambda}_0^t\bar{\Sigma}_0 + \dot{\Lambda}_1^t\bar{\Sigma}_1 + \Lambda_0\dot{\bar{\Sigma}}_0^t + \Lambda_1\dot{\bar{\Sigma}}_1^t\big). \tag{A.29}$$

Note that the nontidal contributions to $\dot{L}_i$ and $\dot{\bar{\Sigma}}_i$ cancel because Λ_i are constant except for the tidal terms. Then we solve for $\dot{\Lambda}_0^t$ and $\dot{\Lambda}_1^t$,

$$\dot{\Lambda}_0^t = \big[(1+j\bar{\Sigma}_1)\dot{L}_0^t - (1-j)\Lambda_0\dot{\bar{\Sigma}}_0^t - (1-j)\Lambda_1\dot{\bar{\Sigma}}_1^t - (1-j)\dot{L}_1^t\bar{\Sigma}_1\big]\big/\big[1 + (1-j)\bar{\Sigma}_0 + j\bar{\Sigma}_1\big]^{-1}, \tag{A.30}$$

$$\dot{\Lambda}_1^t = \frac{(1+(1-j)\bar{\Sigma}_0)\dot{L}_1^t - j\Lambda_0\dot{\bar{\Sigma}}_0^t - j\Lambda_1\dot{\bar{\Sigma}}_1^t - j\dot{L}_0^t\bar{\Sigma}_0}{1 + (1-j)\bar{\Sigma}_0 + j\bar{\Sigma}_1}. \tag{A.31}$$

And finally, from here, we use the definition of $\tilde{a}_i = \sqrt{m_i\mu_i\Lambda_i}$ to get the rate of change of the state variables $\tilde{a}_i$:

$$\frac{\mathrm{d}\tilde{a}_i}{\mathrm{d}t} = 2\frac{\tilde{a}_i}{\Lambda_i}\dot{\Lambda}_i^t. \tag{A.32}$$

The disturbing function coefficients are as follows:

$$C^s_{ee} = C^s_{e'e'} = \frac{1}{8}\big(2D_\alpha b^0_{1/2}(\alpha) + D^2_\alpha b^0_{1/2}(\alpha)\big), \tag{A.33}$$

$$C^s_{ee'} = \frac{1}{4}\big(2b^1_{1/2}(\alpha) - 2D_\alpha b^1_{1/2}(\alpha) - D^2_\alpha b^1_{1/2}(\alpha)\big), \tag{A.34}$$

$$C^r_{e} = \frac{1}{2}\big(-2jb^j_{1/2}(\alpha) - D_\alpha b^j_{1/2}(\alpha)\big), \tag{A.35}$$

$$C^r_{e'} = \frac{1}{2}\big((2j-1)b^{j-1}_{1/2}(\alpha) + D_\alpha b^{j-1}_{1/2}(\alpha)\big) - 2\alpha\delta_{j2}, \tag{A.36}$$

$$C^r_{ee} = \frac{1}{8}\big(\big(-5k+4k^2\big)b^k_{1/2}(\alpha) + (-2+4k)D_\alpha b^k_{1/2}(\alpha) + D^2_\alpha b^k_{1/2}(\alpha)\big), \tag{A.37}$$

$$C^r_{ee'} = \frac{1}{4}\big(\big(-2+6k-4k^2\big)b^{k-1}_{1/2}(\alpha) + (2-4k)D_\alpha b^{k-1}_{1/2}(\alpha) - D^2_\alpha b^{k-1}_{1/2}(\alpha)\big), \tag{A.38}$$

$$C^r_{e'e'} = \frac{1}{8}\big(\big(2-7k+4k^2\big)b^{k-2}_{1/2}(\alpha) + (-2+4k)D_\alpha b^{k-2}_{1/2}(\alpha) + D^2_\alpha b^{k-2}_{1/2}(\alpha)\big), \tag{A.39}$$

where $D_\alpha f = \alpha\,\mathrm{d}f/\mathrm{d}\alpha$, $k = 2j$, and $b^m_l(\alpha)$ are the usual Laplace coefficients (Murray and Harper, 1993). We have evaluated the coefficients at $\alpha = ((j-1)/j)^{2/3}$.

References

Borderies, N., Goldreich, P., 1984. A simple derivation of capture probabilities for the J + 1:J and J + 2:J orbit–orbit resonance problems. Celest. Mech. 32, 127–136.

Brouwer, D., 1959. Solution to the problem of artificial satellite theory without drag. Astron. J. 64, 378–397.

Bulirsch, R., Stoer, J., 1966. Numerical treatment of ordinary differential equations by extrapolation methods. Numer. Math. 8, 93–104.

Callegari, N., Yokoyama, T., 2007. Dynamics of two satellites in the 2/1 mean-motion resonance: Application to the case of Enceladus and Dione. Celest. Mech. Dynam. Astron. 98, 5–30.

Love, A.E.H., 1944. A Treatise on the Mathematical Theory of Elasticity, fifth ed. Dover, New York.

Meyer, J.A., Wisdom, J., 2007a. Tidal heating in Enceladus. Icarus 188, 535–539.

Meyer, J.A., Wisdom, J., 2007b. Episodic volcanism on Io and Enceladus. Icarus, submitted for publication.

Moore, W.B., 2004. Tidal deformation and tidal dissipation in Europa. In: Workshop on Europa's Icy Shell: Past, Present, and Future, Houston, TX, February 6–8, 2004. Abstract No. 7055.

Murray, C.D., Harper, D., 1993. Expansion of the Planetary Disturbing Function to Eighth Order in the Individual Orbital Elements. QMW Maths Notes, vol. 15. University of London, London.

Ojakangas, G.W., Stevenson, D.J., 1986. Episodic volcanism of tidally heated satellites with application to Io. Icarus 66, 341–358.

Peale, S.J., 1986. Orbital resonances, unusual configurations and exotic rotation states among planetary satellites. In: Burns, J., Matthews, M. (Eds.), Satellites. Univ. of Arizona Press, Tucson, pp. 159–223.

Porco, C.C., and 24 colleagues, 2006. Cassini observes the active south pole of Enceladus. Science 311, 1393–1401.

Ross, M.N., Schubert, G., 1989. Viscoelastic models of tidal heating in Enceladus. Icarus 78, 90–101.

Sinclair, A.T., 1972. On the origin of the commensurabilities amongst the satellites of Saturn. Mon. Not. R. Astron. Soc. 160, 169–187.

Sinclair, A.T., 1983. A re-consideration of the evolution hypothesis of the origin of the resonances among Saturn's satellites. In: Markellos, Y.Y., Kozai, Y. (Eds.), Dynamical Trapping and Evolution in the Solar System. Reidel, Dordrecht.

Spencer, J.R., and 9 colleagues, 2006. Cassini encounters Enceladus: Background and the discovery of a south polar hot spot. Science 311, 1401–1405.

Squyres, S.W., Reynolds, R.T., Cassen, P.M., Peale, S.J., 1983. The evolution of Enceladus. Icarus 53, 319–331.

Sussman, G.J., Wisdom, J., 2001. Structure and Interpretation of Classical Mechanics. MIT Press, Cambridge, MA.

Tittemore, W.C., Wisdom, J., 1990. Tidal evolution of the uranian satellites. II. An explanation of the anomalously high orbital inclination of Miranda. Icarus 78, 63–89.

Touma, J., Wisdom, J., 1998. Resonances in the early evolution of the Earth–Moon system. Astron. J. 115, 1653–1663.

Wisdom, J., 2004. Spin–orbit secondary resonance dynamics of Enceladus. Astron. J. 128, 484–491.

Wisdom, J., Holman, M., 1991. Symplectic maps for the N-body problem. Astron. J. 102, 1528–1538.